ISJ 15: 302-315, 2018 ISSN 1824-307X

RESEARCH REPORT

The mRNA expression profiles demonstrating versatile roles of glutathione S-transferase genes in the mollusk *Chlamys farreri*

M Wang[1], L Wang[3,4,5], D Ni[1], Q Yi[3,4,5], X Wang[6], Z Jia[1], L Song[2,3,4,5*]

[1]CAS Key Laboratory of Experimental Marine Biology, Institute of Oceanology, Chinese Academy of Sciences, Qingdao 266071, China
[2]Laboratory for Marine Fisheries Science and Food Production Processes, National Laboratory for Marine Science and Technology, Qingdao 266237, China
[3]Liaoning Key Laboratory of Marine Animal Immunology, Dalian Ocean University, Dalian 116023, China
[4]Liaoning Key Laboratory of Marine Animal Immunology and Disease Control, Dalian Ocean University, Dalian 116023, China
[5]Dalian Key Laboratory of Disease Prevention and Control for Aquaculture Animals, Dalian Ocean University, Dalian 116023, China
[6]College of Marine Science and Biological Engineering, Qingdao University of Science & Technology, Qingdao 266042, China

Accepted August 27, 2018

Abstract

Glutathione S-transferase (GST) is a superfamily of multifunction enzymes with varying catalytic roles in cellular detoxification to protect hosts against oxidative damage. In the present study, six GST genes were identified from *Chlamys farreri*, including *Cf*GSTω, *Cf*GSTσ-1, *Cf*GSTσ-2, *Cf*GSTρ, *Cf*GSTζ and *Cf*mGST. *Cf*GSTs shared high similarities with their counterparts from other species, and were clustered with their homologues into the corresponding clades in the phylogenetic tree, respectively. We investigated the distribution of their mRNA transcripts in different tissues and their temporal expression profiles in hemocytes after microbe stimulations by quantitative real-time PCR. The six *Cf*GST genes were detectable in all the tested tissues, including hemocytes, muscle, mantle, gill, hepatopancreas, and gonad. Stimulations with various microbes drastically induced the mRNA transcripts of all the *Cf*GSTs with different expression profiles. For examples, *Cf*GSTω could be induced by three kinds of microbes, including *Vibrio anguillarum*, *Micrococcus luteus* and *Pichia pastoris*, whereas *Cf*mGST could be only induced by *V. anguillarum.* These results indicated a powerful detoxification system of GSTs in scallop. Moreover, the distinct mRNA expression profiles of *Cf*GSTs indicated their versatile and immune-challenge specific roles in the mollusk *C. farreri*.

Key Words: *Chlamys farreri*; Glutathione S-transferase; innate immunity

Introduction

The innate immunity acts as the first defense line for all multicellular animals and almost the only mechanism for invertebrates to protect themselves against microbial invaders (Hoffmann *et al*., 1999). Many innate immune responses, especially hemocytes-mediated phagocytosis, were accompanied with respiratory burst and followed by mass production of reactive oxygen species (ROS) (Liu *et al*., 2009; Jia *et al*., 2018). The production of ROS is an effective way to eliminate invading microbes; however, it has been already proved to be a double-edged sword (Benedetti *et al*., 2015). Low concentration of ROS is beneficial for activating signaling pathways mediating various responses to kill or eliminate foreign invaders (He and Klionsky, 2009). While extremely high levels of ROS may be detrimental to biological macromolecules, and lead to cellular dysfunctions, increase cell damage and finally threaten hosts' survival (Martindale and Holbrook, 2002). Therefore, almost all the aerobic organisms have developed an antioxidant system to remove excessive ROS and maintain the redox balance (Halliwell, 2006). The antioxidant system is constituted by a series of antioxidant enzymes, such as superoxide dismutase (SOD), catalase (CAT), peroxiredoxin (PRX), thioredoxin peroxidase (TPX), thioredoxin reductase (TRX), glutathione peroxidase (GPX), glutathione reductase (GRX),

Corresponding author:
Linsheng Song
Dalian Ocean University
Dalian 116023, China
E-mail: lshsong@dlou.edu.cn; lshsong@qdio.ac.cn

glutathione-S-transferase (GST) and many other non-enzymatic antioxidant molecules (Harris, 1992).

Among all these antioxidant enzymes, GST (EC: 2.5.1.18) is a superfamily of multifunction enzymes, which play varying catalytic roles in cellular detoxification and protect hosts from oxidative damage (Strange *et al*., 2001). By now, at least 15 different classes of GSTs have been identified and characterized in numerous organisms according to their structural, catalytic and immune features, including alpha (α), beta (β), delta (δ), epsilon (ε), kappa (κ), lambda (λ), mu (μ), omega (ω), phi (φ), pi (π), sigma (σ), tau (τ), theta (θ), zeta (ζ) and rho (ρ) (Hayes *et al*., 2005). The microsomal GSTs, members of the membrane associated protein in eicosanoid and glutathione metabolism (MAPEG) protein family, also play pivotal roles in antioxidant reaction (Morgenstern *et al*., 1982). Although no criteria were developed to classify GSTs in marine organisms, the expression profiles and enzyme activities of GSTs have been investigated in some aquatic species, such as abalone *Haliotis diversicolor* (Ren *et al*., 2009), bay scallop *Argopecten irradians* (Wang *et al*., 2017a), disk abalone *Haliotis discus discus* (Wan *et al*., 2008; Sandamalika *et al*., 2018), green-lipped mussels *Perna viridis* (Li *et al*., 2013), intertidal copepod *Tigriopus japonicas* (Lee *et al*., 2007), manila clam *Venerupis philippinarum* (Xu *et al*., 2010; Li *et al*., 2012; Zhang *et al*., 2012a,b; Li *et al*., 2015), marine mussels *Mytilus galloprovincialis* (Wang *et al*., 2013; Li *et al*., 2015), pearl oyster *Pinctada martensii* (Chen *et al*., 2011), razor clam *Solen grandis* (Yang *et al*., 2012), ridge-tail white prawn *Exopalaemon carinicauda* (Duan *et al*., 2013), and sea cucumber *Apostichopus japonicas* (Shao *et al*., 2017; Zhang *et al*., 2017a,b). Some of these GSTs from aquatic species were involved in innate immunity and could respond to invading microbes, for examples, the sigma class GST from *H. diversicolor* was significantly induced post bacteria challenged (Ren et al., 2009), while the mRNA expression level of a GST gene in *S. grandis* was significantly up-regulated in hemocytes after being stimulated by β-1, 3-glucan (Yang *et al*., 2012).

The Zhikong scallop *Chlamys farreri* is one of the most important commercial species which is widely cultivated in the northern coastal provinces of China (Li *et al*., 2015b; Song *et al*., 2015). With the rapid expansion of intensive culture and environmental deterioration, scallops have frequently suffered from various diseases. The knowledge about the antioxidant system and its function in response to invading microbes may provide a better understanding of innate immune mechanisms in scallop and potential development of disease control strategies in scallop farming. In previous reports, several antioxidant enzyme genes have been identified and investigated in *C. farreri*, such as SOD (Ni et al., 2007; Wang *et al*., 2018), CAT (Li *et al*., 2008), PRX (Cong *et al*., 2009), and GPX (Mu *et al*., 2010). Moreover, the cDNA sequence of a pi (π) class GST and its expression profiles in response to Benzo[α]pyrene exposure was also reported in *C. farreri* (Miao *et al*., 2011). However, compared with other antioxidant enzymes in scallop, the information of GSTs is rather rare and fragmentary and more investigation is needed to illustrate their exact roles in the innate immunity. In the present study, six novel GST genes were identified in *C. farreri* based on the analysis of expression sequence tag (EST) sequences (Wang *et al*., 2009) with the main objectives (1) to characterize the molecular features of *Cf*GST genes (2) to detect the tissue distribution and temporal mRNA expression profiles of their mRNA transcripts, and (3) to compare these features to lead a better understanding of their versatile roles in *C. farreri*.

Materials and methods

Scallops, immune stimulation and sample collection

Adult scallops with an average 55 mm in shell length were collected from a local farm in Qingdao, China, and maintained in aerated seawater at about 15 °C. Approximately 120 scallops were employed for microbe stimulation assay. After acclimated for two weeks, 30 scallops were kept in tanks containing live *Vibrio anguillarum* strain M3 (kindly provided by Prof. Zhaolan Mo) at a final concentration of 1.0×10^8 colony forming units (CFU) mL^{-1}, and defined as Gram-negative bacteria stimulation group. Another 30 scallops were transferred to the tanks containing live *Micrococcus luteus* (28001, Microbial Culture Collection Center, China) at a final concentration of 1.0×10^8 CFU mL^{-1}, and defined as Gram-positive bacteria stimulation group. The third 30 scallops were transferred to the fungi-containing tanks with live *Pichia pastoris* strain GS115 (PA17237, Thermo Fisher Scientific, USA) at a final concentration of 1.0×10^8 CFU mL^{-1}, and defined as fungi stimulation group. And the last 30 scallops were employed as the control group. Five individuals from each group were randomly sampled at 0, 3, 6, 12, 24 and 48 hours post stimulation (hps), respectively. The hemolymphs were collected from the adductor muscle using syringes and centrifuged at 800 *g*, 4 °C for 10 min to harvest the hemocytes for RNA preparation. Hemocytes, muscle, mantle, gill, hepatopancreas and gonad from five untreated scallops were collected to determine the mRNA transcripts distribution of *Cf*GST genes.

RNA isolation and cDNA synthesis

Raw RNA was isolated from the hemocytes and other tissues of scallops using RNAiso plus reagent (9108, Takara, Japan). The first-strand synthesis was performed with M-MLV (M1705, Promega, USA) using the DNase I (RQ1, M6101, Promega, USA) treated raw RNA as template and adaptor primer-oligo(dT) as primer (Table 1). The reaction were carried out at 42 °C for 1 h, terminated by heating at 95°C for 5 min. A homopolymeric tail was added to the 5` end of the cDNA using terminal deoxynucleotidyl transferase (TdT, 2230, Takara, Japan) and dCTP (U1221, Promega, USA) and the obtained product were subsequently stored at -80 °C till use.

cDNA cloning of the full-length Cf*GST genes*

The full-length cDNA sequences of *Cf*GST genes were obtained by rapid-amplification of cDNA ends (RACE) technique based on the analysis of EST sequences (Wang *et al*., 2009). All the primers

used in this assay were listed in Table 1. All PCR amplification was performed in a TP-600 PCR Thermal Cycler (Takara, Japan). The PCR products were gel-purified and then cloned into the pMD19-T simple vector (3271, Takara, Japan), and then transformed into the competent cells *Escherichia coli* strain Top10 (CB104, Tiangen, China). The positive recombinants were identified through anti-Ampicillin selection and verified via PCR screening with sequencing primers M13-47 and RV-M (Table 1). Five positive clones were sequenced with a 3730XL automated sequencer (Thermo Fisher Scientific, USA).

Bioinformatics analysis of sequences

The search for protein sequence similarity was conducted with blast+ 2.2.18. The deduced amino acid sequences were analyzed with DNAStar Lasergene suite 7.1.0.44 using the EditSeq module. SignalP 3.0 was employed to predict the presence and location of signal peptide. The protein domain and motif features were predicted by Simple Modular Architecture Research Tool (SMART) 5.1. A phylogenic NJ tree was constructed with MEGA 5.05. To derive confidence value for the phylogeny analysis, bootstrap trials were replicated 1000 times.

Real-time PCR analysis of relative mRNA expression levels

The mRNA expression profiles of *Cf*GST genes were detected via quantitative real-time PCR (qRT-PCR). All qRT-PCR reactions were performed with the SYBR premix Ex Taq (Tli RNaseH Plus, RR420, Takara, Japan) in a 7500 Real-Time Detection System (Thermo Fisher Scientific, USA). All the primers used in qRT-PCR assay were listed in Table 1. The mRNA expression leveld of *Cf*GST genes were normalized to that of elongation factor 1 α (EF-1α) gene for each sample, according to our previous reports (Wang *et al*., 2016b, 2017b). The comparative C_T method ($2^{-\Delta\Delta Ct}$ method) was used to analyze the relative mRNA expression level of GST genes (Schmittgen and Livak, 2008). All data were given as means ± S.D. (n = 5). The data were subjected to one-way analysis of variance (one-way ANOVA) followed by a multiple comparison via IBM SPSS Statistics 19.0.0.0, and the *p* values less than 0.05 were considered statistically significant.

Table 1 Primers used in the present research

Primer	Sequence (5`-3`)	Brief information
*Cf*GSTω-Race-F1	GGTAATGAAGTCGCTGCCTGCTGT	Gene specific primer for 3` RACE
*Cf*GSTω-Race-F2	CTTTTATAAAAGTTACGCAGCAGG	Gene specific primer for 3` RACE
*Cf*GSTω-Race-R1	AAAGGACAGAACCTCATGCTATACAGC	Gene specific primer for 5` RACE
*Cf*GSTω-Race-R2	GAATCTTTAGAGTGTGATTTGAGA	Gene specific primer for 5` RACE
*Cf*GSTσ-1-Race-F1	GCTGACCGAGTTCTTTAAGTA	Gene specific primer for 3` RACE
*Cf*GSTσ-1-Race-F2	TAAGAAGAAAACTTTCGATTCAGT	Gene specific primer for 3` RACE
*Cf*GSTσ-2-Race-F1	ACTTCGAAAGTGACGAGACTAAGAAGG	Gene specific primer for 3` RACE
*Cf*GSTσ-2-Race-F2	CTATTCCTAAGTTTGCCAAAATCTTCACAA	Gene specific primer for 3` RACE
*Cf*GSTσ-2-Race-R1	CAAGTACCGGCAGCTGACCAGTGGGCATCTTTT	Gene specific primer for 5` RACE
*Cf*GSTσ-2-Race-R2	TAATGGTATCTTCTTCGAATGTTTGCCCGG	Gene specific primer for 5` RACE
*Cf*GSTρ-Race-F1	CAGTTTGCTTATGGGGATAAGTTCACT	Gene specific primer for 3` RACE
*Cf*GSTρ-Race-F2	GCCACTGTGGTACGATTTGGCTGCGACATA	Gene specific primer for 3` RACE
*Cf*GSTζ-Race-F1	GGCTGATGCGTGTCTGGTTCCTCAGGT	Gene specific primer for 3` RACE
*Cf*GSTζ-Race-F2	GAAACAGTTCCCTACCATTGCTCGTCTAAA	Gene specific primer for 3` RACE
*Cf*GSTζ-Race-R1	ACCTGAGGAACCAGACACGCATCAGCCATTGTC	Gene specific primer for 5` RACE
*Cf*GSTζ-Race-R2	CCATTCCATTTTACACCTCGTCCC	Gene specific primer for 5` RACE
*Cf*mGST-Race-F1	GGAATGTAAACCAACGTTATCGGACCC	Gene specific primer for 3` RACE
*Cf*mGST-Race-F2	GGATCCGGCAACAGCCCTGATGTACTT	Gene specific primer for 3` RACE
*Cf*mGST-Race-R1	GGTCCGATAACGTTGGTTTACATTCCT	Gene specific primer for 5` RACE
*Cf*mGST-Race-R2	GGTTAGCGTACACCGACTTTCGAA	Gene specific primer for 5` RACE
*Cf*GSTω-qRT-F	TCGTTAGAGTAACCACCAGGA	Gene specific primer for real-time PCR
*Cf*GSTω-qRT-R	ATGCTATACAGCCTTAGTTTCCC	Gene specific primer for real-time PCR
*Cf*GSTσ-1-qRT-F	AGTTTGGTTTGGCGGGAG	Gene specific primer for real-time PCR
*Cf*GSTσ-1-qRT-R	TGCGTACTTAAAGAACTCGGTC	Gene specific primer for real-time PCR
*Cf*GSTσ-2-qRT-F	CACCACCATCTATCTAAGGACAC	Gene specific primer for real-time PCR
*Cf*GSTσ-2-qRT-R	GTATCTTCTTCGAATGTTTGCCC	Gene specific primer for real-time PCR
*Cf*GSTρ-qRT-F	TACCAAGACTCCAAGCCTACTACGA	Gene specific primer for real-time PCR
*Cf*GSTρ-qRT-R	GTCCTTCAATTCTCCTTCCAGCCA	Gene specific primer for real-time PCR
*Cf*GSTζ-qRT-F	GAGATAAGGTGACAATGGCGG	Gene specific primer for real-time PCR
*Cf*GSTζ-qRT-R	TTTAGACGAGCAATGGTAGGGA	Gene specific primer for real-time PCR
*Cf*mGST-qRT-F	TAACCCGGAGGACTGTGCCA	Gene specific primer for real-time PCR
*Cf*mGST-qRT-R	ATGACACCTTCTGATGCGTTCCAC	Gene specific primer for real-time PCR
*Cf*EF-1α-qRT-F	ATCCTTCCTCCATCTCGTCCT	Internal control for real-time PCR
*Cf*EF-1α-qRT-R	GGCACAGTTCCAATACCTCCA	Internal control for real-time PCR
adaptor primer-oligo (dT)	GGCCACGCGTCGACTAGTACT_{17}VN	Olido (dT) primer for cDNA synthetize
adaptor primer	GGCCACGCGTCGACTAGTAC	Anchor primer for 3` RACE
adaptor primer-oligo (dG)	GGCCACGCGTCGACTAGTACG_{10}HN	Anchor primer for 5` RACE
M13-47	CGCCAGGGTTTTCCCAGTCACGAC	Vector primer for sequencing
RV-M	GAGCGGATAACAATTTCACACAGG	Vector primer for sequencing

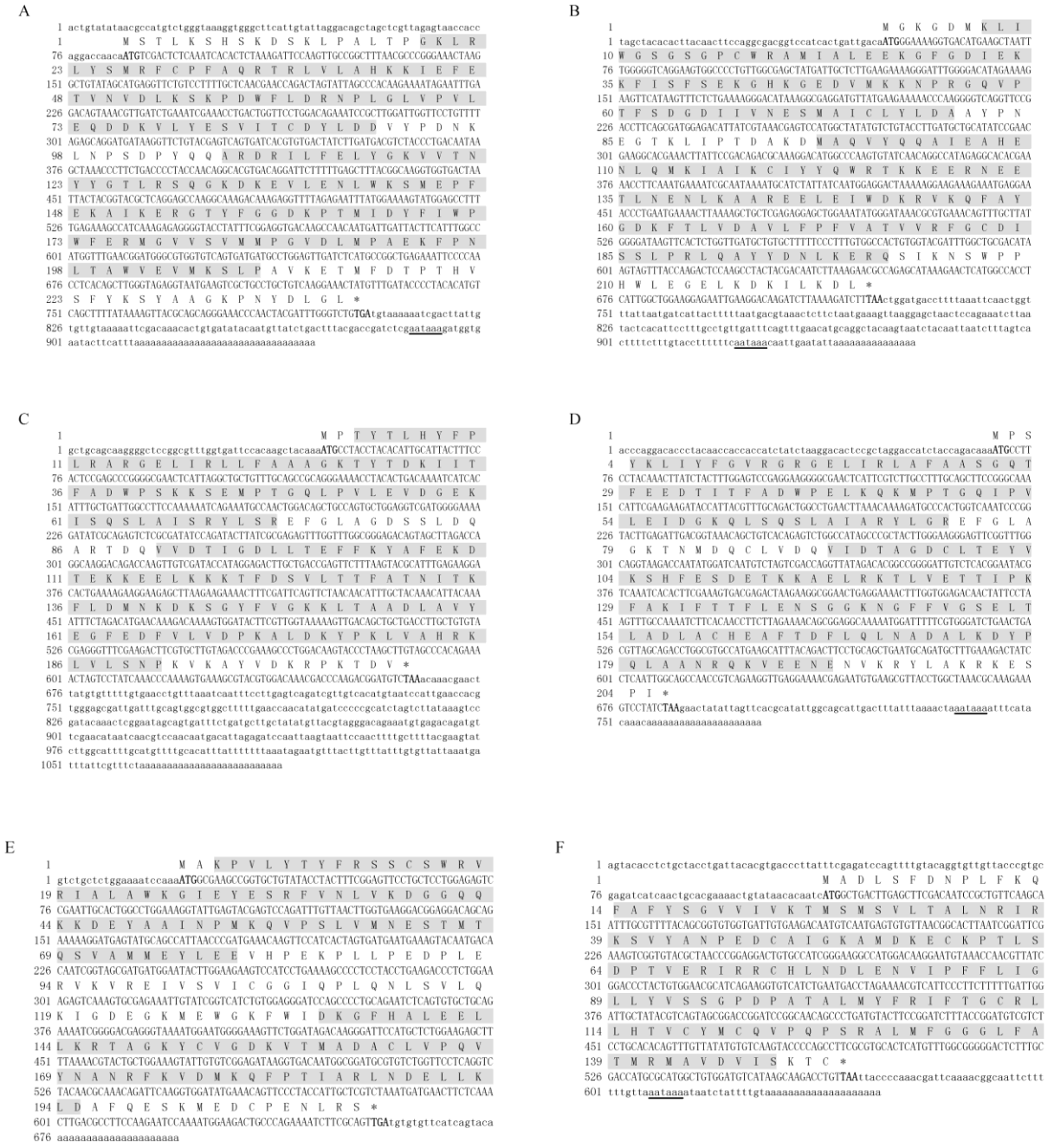

Fig. 1 Nucleotide and deduced amino acid sequences of six *Cf*GSTs (A: *Cf*GSTω, B: *Cf*GSTσ-1, C: *Cf*GSTσ-2, D: *Cf*GSTρ, E: *Cf*GSTζ, F: *Cf*mGST). The nucleotides and amino acids are numbered along the left margin. Capital letters indicated coding sequence, small letters indicated UTRs. The GST_N/GST_C/MAPEG domains are in shade. The single typical polyadenylation signal was underlined. The asterisk and bold font indicated the stop codon

Results

Identification and classification of Cf*GSTs genes*

Six different *Cf*GST genes were identified from the EST database and the full-length cDNA sequences were obtained via RACE technique. Based on the deduced protein sequences identities and phylogenetic analysis with other GSTs, the *Cf*GSTs were classified into five classes, including two in sigma (*Cf*GSTσ-1 and *Cf*GSTσ-2) and one each in omega (*Cf*GSTω), rho (*Cf*GSTρ), zeta (*Cf*GSTζ) and the microsomal GST isoenzyme (*Cf*mGST), respectively. The main sequence features of these GST genes were illustrated in Figure 1 and Table 2. The cDNA sequences of these six *Cf*GST genes were deposited to GenBank

Table 2 Sequence features of the six GSTs in scallop

Feature	*Cf*GSTω	*Cf*GSTσ-1	*Cf*GSTσ-2	*Cf*GSTρ	*Cf*GSTζ	*Cf*mGST
Accession Number	GQ240291	EU183306	GQ240292	EU183305	GU361617	GQ403696
EST	cl23ct28cn28	cl124ct131cn139	cl327ct342cn359	cl51ct57cn59	rscag0_004919	rscag0_001764
cDNA length (bp)	945	1089	776	954	696	647
5` UTR length (bp)	85	46	68	48	21	112
3` UTR length (bp)	140	425	90	231	39	79
ORF length (bp)	720	618	618	675	636	456
Polyadenylation signal sites	1	1	0	1	0	1
Deduced polypeptide length (aa)	239	205	205	224	211	151
Domain information	GST_N+ GST_C	GST_N+ GST_C	GST_N+ GST_C	GST_N+ GST_C	GST_N+ GST_C	MAPEG
Calculated molecular mass (kDa)	27.65	23.22	23.02	25.76	24.20	16.86
Theoretical isoelectric point	7.261	8.849	5.339	6.201	6.417	8.386
Best hits by blastX (protein, taxa, E_value, Score, Identity)	GSTω-2, [*Haliotis discus discus*], 1e-90, 279, 57%	GSTσ, [*Argopecten irradians*], 2e-59, 199, 52%	GSTσ, [*Argopecten irradians*], 6e-114, 334, 78%	GSTρ, [*Solea senegalensis*], 4e-54, 185, 45%	GSTζ, [*Cyprinus carpio*], 1e-84, 259, 59%	mGST-1, [*Xenopus tropicalis*], 4e-45, 156. 52%

database under the following accession numbers: GQ240291 (*Cf*GSTω), EU183306 (*Cf*GSTσ-1), GQ240292 (*Cf*GSTσ-2), EU183305 (*Cf*GSTρ), GU361617 (*Cf*GSTζ) and GQ403696 (*Cf*mGST). *Cf*mGST consisted of an open reading frame (ORF) of 456 bp encoding a polypeptide of 151 amino acid residues with the calculated molecular mass of 16.86 kDa, while *Cf*GSTω, *Cf*GSTσ-1, *Cf*GSTσ-2, *Cf*GSTρ and *Cf*GSTζ consisted of 239, 205, 205, 224 and 211 amino acid residues, respectively. Among these five cytosolic *Cf*GSTs, *Cf*GSTω had the highest calculated molecular mass (27.65 kDa) and *Cf*GSTSσ-2 had the lowest one (23.02 kDa), which were consistent with most identified mammalian GSTs with the calculated molecular mass ranging from 23 kDa to 28 kDa as heterodimers or homodimers. The theoretical isoelectric points of these six putative *Cf*GSTs proteins were calculated from 5.339 to 8.849. These six *Cf*GSTs were annotated using blastx algorithm and each of them showed high identities (from 45% to 78%) with those from other vertebrate or invertebrate species. The assignment of six *Cf*GSTs to the omega, sigma, rho, zeta and microsomal GST isoenzymes was clearly supported by the phylogenetic analysis of all these six *Cf*GSTs along with those previous identified ones from other vertebrate and invertebrate species. These six *Cf*GSTs were separated into five groups in the phylogenetic tree and each GST class formed their own clades (Fig. 2).

Tissue distribution of Cf*GSTs mRNA*

The tissue-specific expression patterns of these six *Cf*GSTs mRNA transcripts have been investigated in the present study. These six *Cf*GST genes were detectable in all the examined tissues, including hemocytes, muscle, mantle, gill, hepatopancreas and gonad, although there were noticeable variations in the mRNA expression levels among different tissues. The highest mRNA expression levels of *Cf*GSTω, *Cf*GSTσ-1 and *Cf*GSTζ were found in hemocytes (Fig. 3A,B,E), *Cf*GSTρ and *Cf*mGST were found to be most abundantly expressed in hepatopancreas (Fig. 3D,F), while the *Cf*GSTσ-2 mRNA transcripts highest expressed in gill (Fig. 3C). Moreover, the mRNA abundance of different *Cf*GSTs was also variable within one single tissue, *Cf*GSTσ-1 was the most abundant GST in hemocytes, while *Cf*GSTρ was the most scarce one (Fig. 4).

Expression profiles of the Cf*GSTs genes after* V. anguillarum *stimulation*

The mRNA transcripts of *Cf*GSTs exhibited differential expression profiles post *V. anguillarum* stimulation (Fig. 5). The relative mRNA expression levels of *Cf*GSTω, *Cf*GSTσ-1, *Cf*GSTσ-2, *Cf*GSTζ and *Cf*mGST were all significant up-regulated within 3 or 6 hps and reached to the peak at 12 hps, which was 26.18-fold, 13.19-fold, 23.08-fold, 18.28-fold and 15.81-fold of the origin levels ($p < 0.05$), respectively (Figure 5A, B, C, E and F), while no significant change was observed in the mRNA expression profiles of *Cf*GSTρ during *V. anguillarum* stimulation (Fig. 5D). Additionally, within the two sigma class *Cf*GSTs, the immune responses of *Cf*GSTσ-2 were more rapidly and intensely than those of *Cf*GSTσ-1 (Fig. 5B,C).

Expression profiles of the Cf*GSTs genes after* M. luteus *stimulation*

The *M. luteus* stimulation affected the mRNA expression profiles of these six *Cf*GSTs differentially

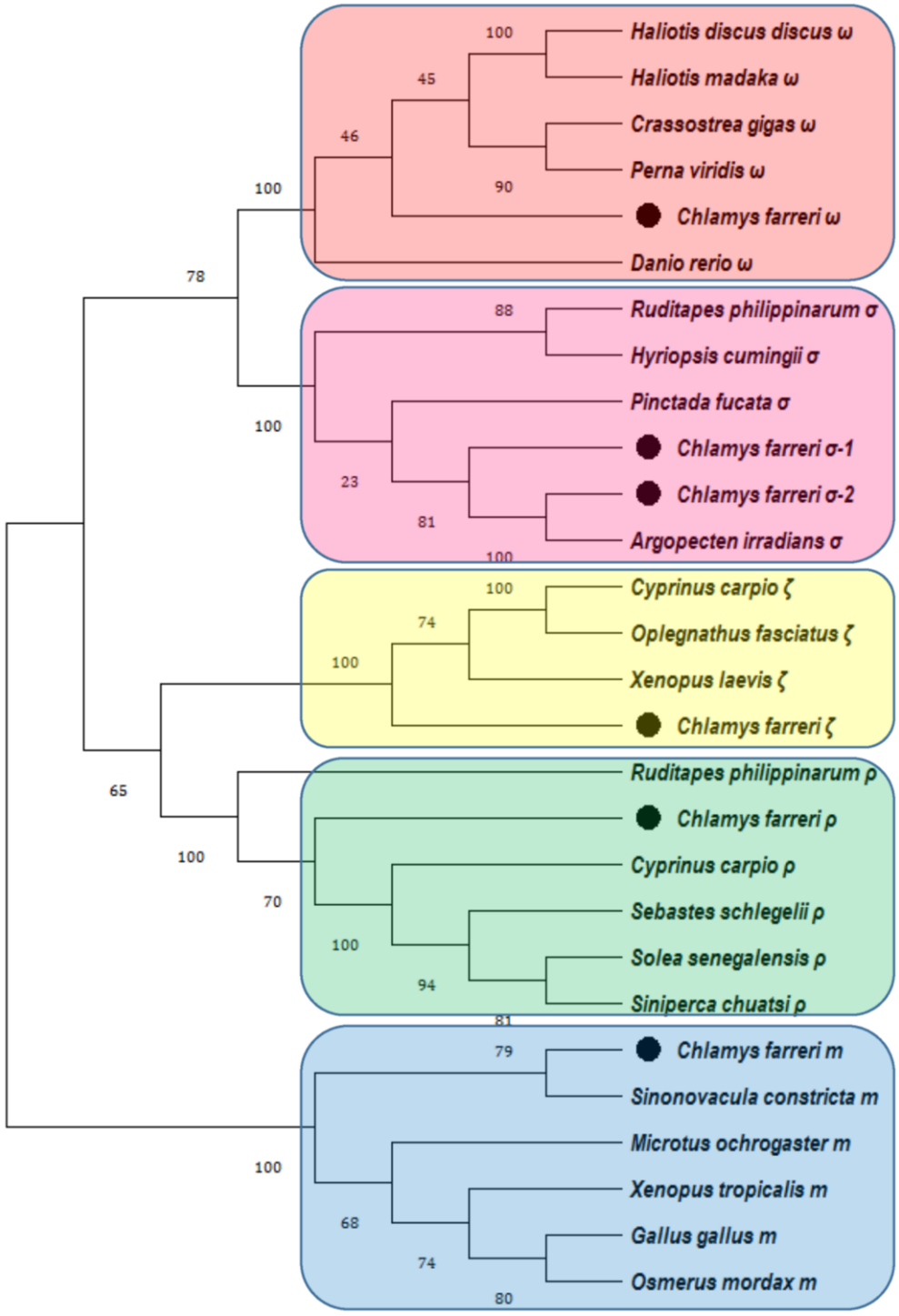

Fig. 2 Consensus phylogenetic analysis based on the amino acid sequences of GSTs from different organisms. The evolutionary history was inferred using the Neighbor-Joining method. The bootstrap consensus tree inferred from 1000 replicates was taken to represent the evolutionary history of the taxa analyzed. All positions containing gaps and missing data were eliminated. The numbers at the forks indicated the bootstrap values. The dark circles stood for sequences from *C. farreri*. The sequences and their accession numbers are as follows, omega class: *Chlamys farreri* (ADF32018), *Crassostrea gigas* (XP_011429380), *Danio rerio* (NP_001002621), *Haliotis discus discus* (ABO26600), *Haliotis madaka* (ALU63761), *Perna viridis* (AGN03944); sigma class: *Argopecten irradians* (ANG56313), *C. farreri* (ACF25904), *C. farreri* (ADF32019); *Hyriopsis cumingii* (AGU68336), *Pinctada fucata* (JAS04242), *Ruditapes philippinarum* (AEW46325); rho class: *C. farreri* (ACF25903); *Cyprinus carpio* (BAS29983); *Ruditapes philippinarum* (AEW46331); *Sebastes schlegelii* (ANW83217); *Siniperca chuatsi* (ACI32418); *Solea senegalensis* (BAG12568); zeta class: *Chlamys farreri* (ADD82544); *Cyprinus carpio* (BAS29981); *Oplegnathus fasciatus* (ADY80028); *Xenopus laevis* (XP_018084636); microsomal: *C. farreri* (ADF45336), *Gallus gallus* (NP_001129022), *Microtus ochrogaster* (XP_005364596), *Osmerus mordax* (ACO10098), *Sinonovacula constricta* (ALC77324), *Xenopus tropicalis* (NP_001011245)

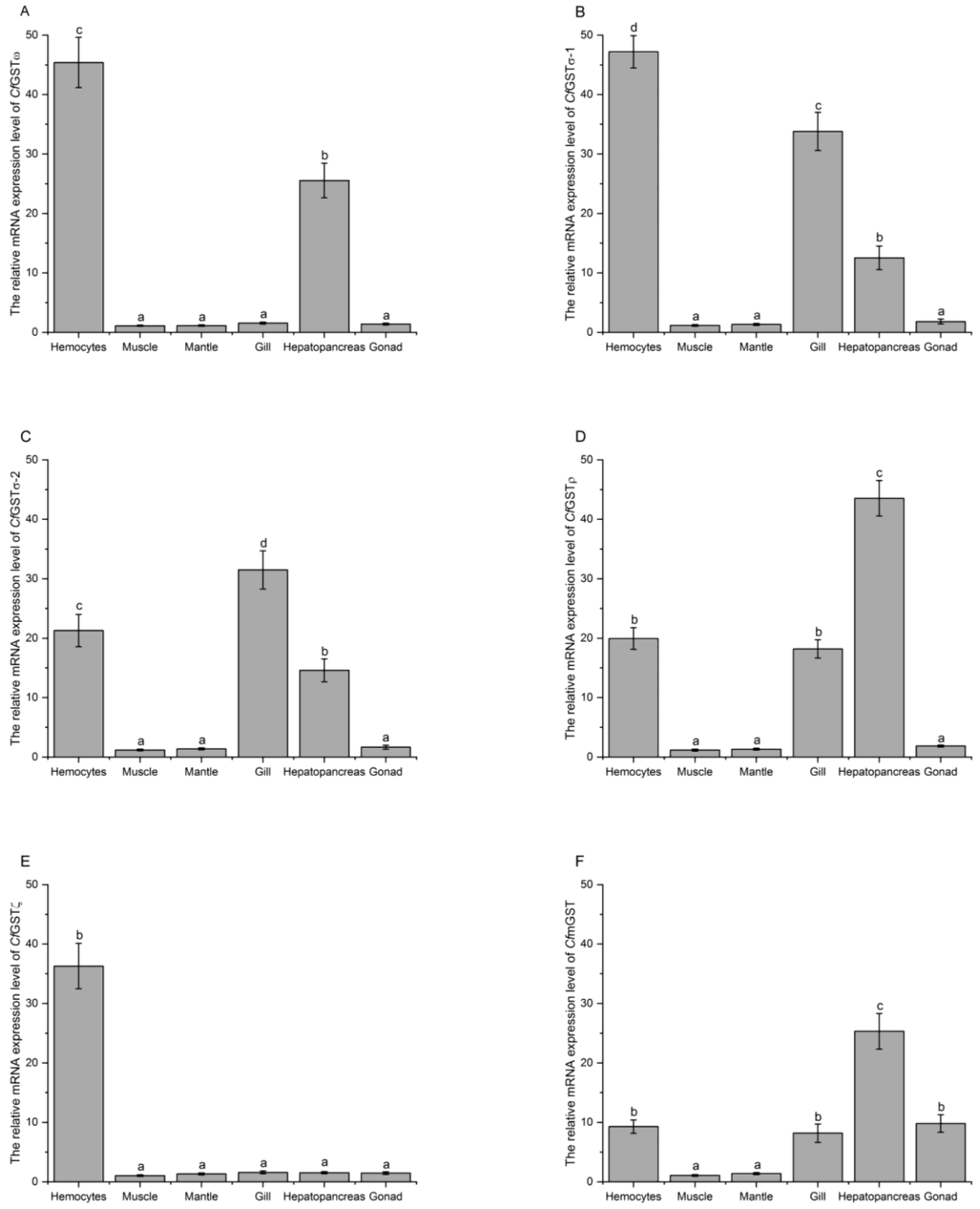

Fig. 3 Tissue distribution of six *Cf*GSTs mRNA transcripts detected by qRT-PCR (A: *Cf*GSTω, B: *Cf*GSTσ-1, C: *Cf*GSTσ-2, D: *Cf*GSTρ, E: *Cf*GSTζ, F: *Cf*mGST). The mRNA expression level of *Cf*GSTs in hemocytes, mantle, gill, hepatopancreas and gonad were normalized to that of muscle. Vertical bars represented mean ± S.D. (n = 5), and bars with different characters indicated significantly different ($p < 0.05$)

(Fig. 6). The relative mRNA expression levels of *Cf*GSTω and *Cf*GSTρ were all significant up-regulated within 3 hps and reached to the peak at 6 hps, which was 27.03-fold and 28.73-fold of the origin levels ($p < 0.05$), respectively (Fig. 6A,D), and those of *Cf*GSTζ were significant up-regulated at 6 hps and reached the peak at 12 hps (15.18-fold, $p < 0.05$, Fig. 6E). While no significant difference in *Cf*GSTσ-1, *Cf*GSTσ-2 and *Cf*mGST mRNA expression was observed (Fig. 6B,C,F).

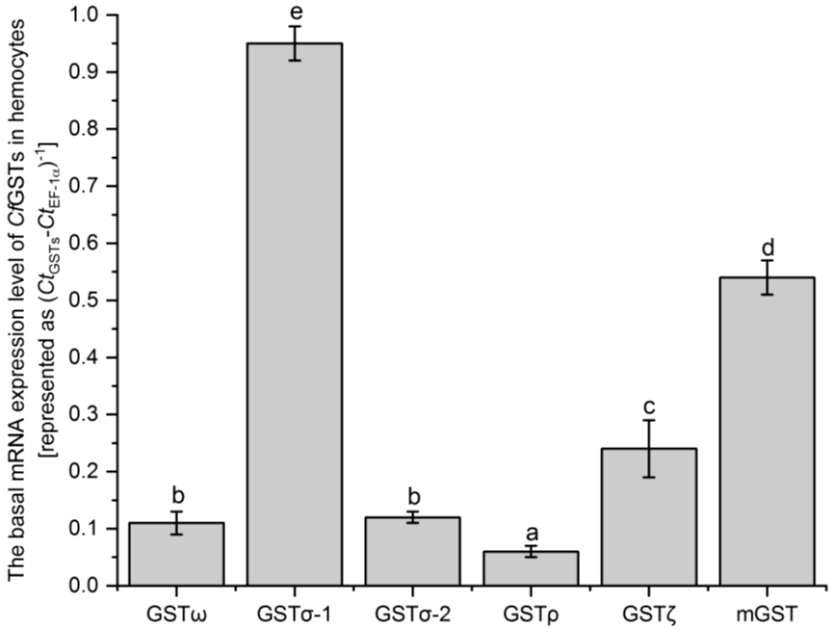

Fig. 4 Quantification of abundance of different *Cf*GST isoforms in hemocytes of untreated scallops. The abundance were calculated relative to EF-1α gene and shown as $(Ct_{GSTs}\text{-}Ct_{EF\text{-}1\alpha})^{-1}$. Vertical bars represented mean ± S.D. (n = 5), and bars with different characters indicated significant difference ($p < 0.05$)

Expression profiles of the Cf*GSTs genes after* P. pastoris *stimulation*

Only two *Cf*GSTs, *Cf*GSTρ and *Cf*GSTζ, were drastically induced during *P. pastoris* stimulation (Fig. 7). The mRNA expression level of *Cf*GSTρ was significantly up-regulated firstly at 3 hps (4.94-fold, $p < 0.05$) and then reached to the peak expression level at 6 hps, which was 18.36-fold of the origin levels ($p < 0.05$, Fig. 7D). While the *Cf*GSTζ were significantly induced at 6 hps (6.53-fold, $p < 0.05$) and reached its highest expression level at 12 hps (18.78-fold, $p < 0.05$, Fig. 7E). Although these six *Cf*GSTs expressions in the normal group were slightly fluctuant throughout the experiment, no significant difference was observed (Figs 5,6,7).

Discussion

Glutathione S-transferases are a well characterized protein family of multifunctional isoenzymes ubiquitously identified in many aerobic organisms from bacteria to animals, and play pivotal roles in the oxidative stress responses and detoxification pathways (Hayes *et al*., 2005). In the present study, the full-length cDNA sequences of six different GST genes, including *Cf*GSTω, *Cf*GSTσ-1, *Cf*GSTσ-2, *Cf*GSTρ, *Cf*GSTζ and *Cf*mGST, were identified from *C. farreri*. Their sequence features, high similarities with other previous identified GTSs and the phylogenetic relationship collectively suggested that they are novel invertebrate GSTs and may have similar function with GSTs from other invertebrates.

In the GST family, at least 15 different classes of GSTs have been identified and characterized in numerous aerobic organisms according to their different primary structures, enzyme properties, physiological functions and immune activities (Strange *et al*., 2001). According to their functional differences, GST isoforms would express differentially in various tissues. Accumulating research achievements on tissue-specific expression profiles of GSTs in aquatic organisms have revealed that GSTs are generally abundantly expressed in the mantle, gills, hepatopancreas and gonad (Li *et al*., 2008; Ren *et al*., 2009; Mu *et al*., 2010; Xu *et al*., 2010; Chen *et al*., 2011; Li *et al*., 2012; Yang *et al*., 2012; Zhang *et al*., 2012a; Duan *et al*., 2013; Li *et al*., 2013; Wang *et al*., 2013; Shao *et al*., 2017), indicating that different tissue-specific expression pattern of GSTs were associated with their differential susceptibility to antioxidant damage. In the present study, the mRNA transcripts of the six *Cf*GST genes could be detected in all tested tissues, including hemocytes, muscle, mantle, gill, hepatopancreas and gonad, suggesting that they would be involved in many crucial physiologic or immune processes of scallop. And, there were noticeable variations in the tissue-specific expression pattern of *Cf*GSTs. Hemocytes have been demonstrated to play irreplaceable roles in the innate immune response of invertebrates mainly through phagocytosis, which was usually companied with oxidative stress, and tubules of gill filaments were confirmed to be the hematopoietic position in Mollusks (Li *et al*., 2017a). In the present study, almost all the six *Cf*GSTs were high expressed in hemocytes, and *Cf*GSTσ-1, *Cf*GSTσ-2, *Cf*GSTρ and

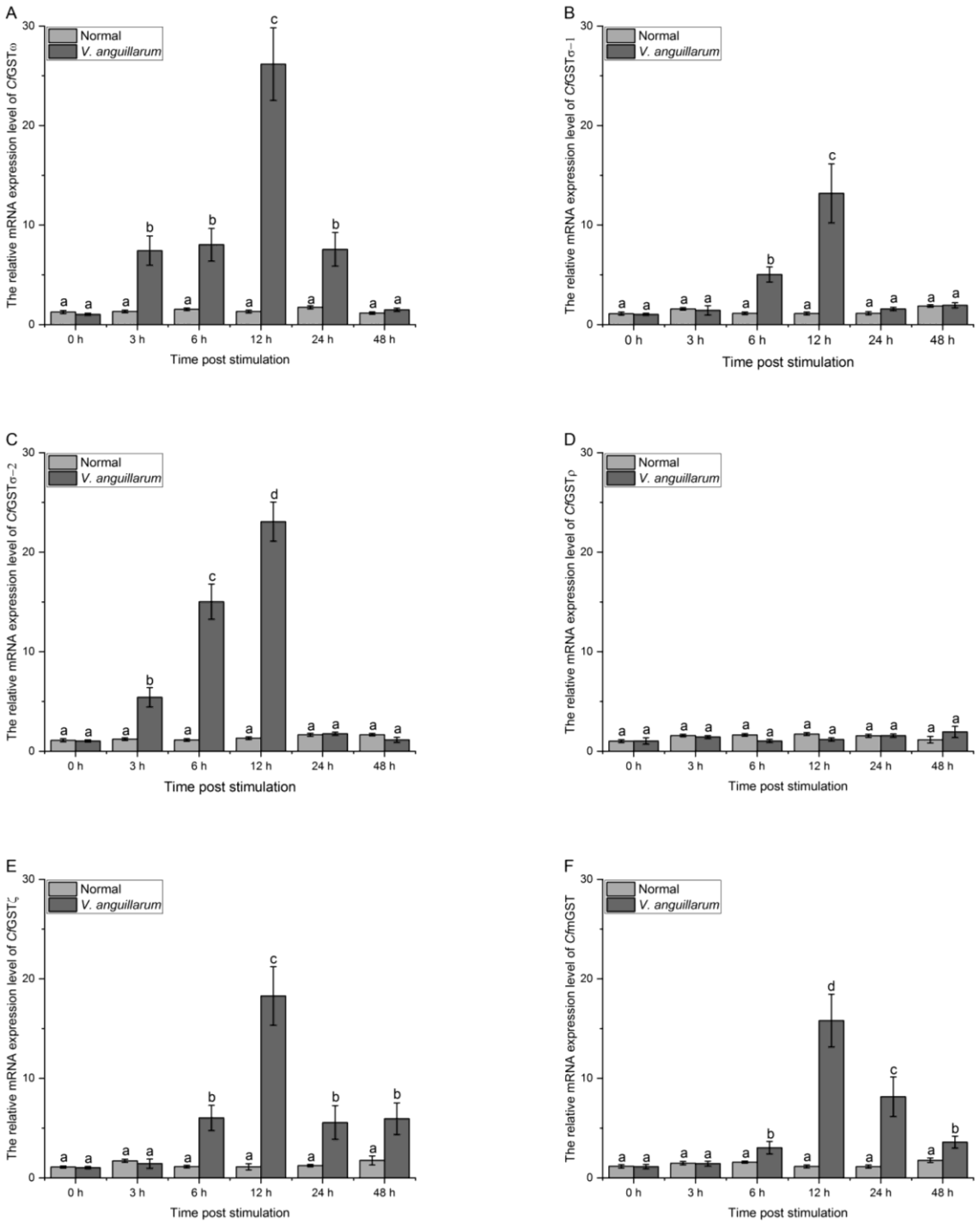

Fig. 5 Temporal mRNA expression profiles of six *Cf*GSTs detected by qRT-PCR in scallop hemocytes post *V. anguillarum* stimulation (A: *Cf*GSTω, B: *Cf*GSTσ-1, C: *Cf*GSTσ-2, D: *Cf*GSTρ, E: *Cf*GSTζ, F: *Cf*mGST). Each values was shown as mean ± S.D. (n = 5), and bars with different characters indicated significant difference ($p < 0.05$)

*Cf*mGST were found to be most abundantly expressed in gills, indicating that these GSTs would act as efficient immune effectors in scallop. While *Cf*GSTω, *Cf*GSTσ-1, *Cf*GSTσ-2, *Cf*GSTρ and *Cf*mGST were highly expressed in hepatopancreas, which was consistent with the opinion that hepatopancreas was the major organ for detoxification of xenobiotics in marine invertebrates (Doi *et al*., 2004). Similar phenome has been observed in *M. galloprovincialis*, in which tissue distribution study revealed that *Mg*GSTa, *Mg*GSTS2, *Mg*GSTS3 transcripts were highly expressed in hemocytes, while *Mg*GSTS1 mRNA was most abundantly expressed in hepatopancreas. Additionally, previous reports have demonstrated that some low constitutively expressed GSTs might

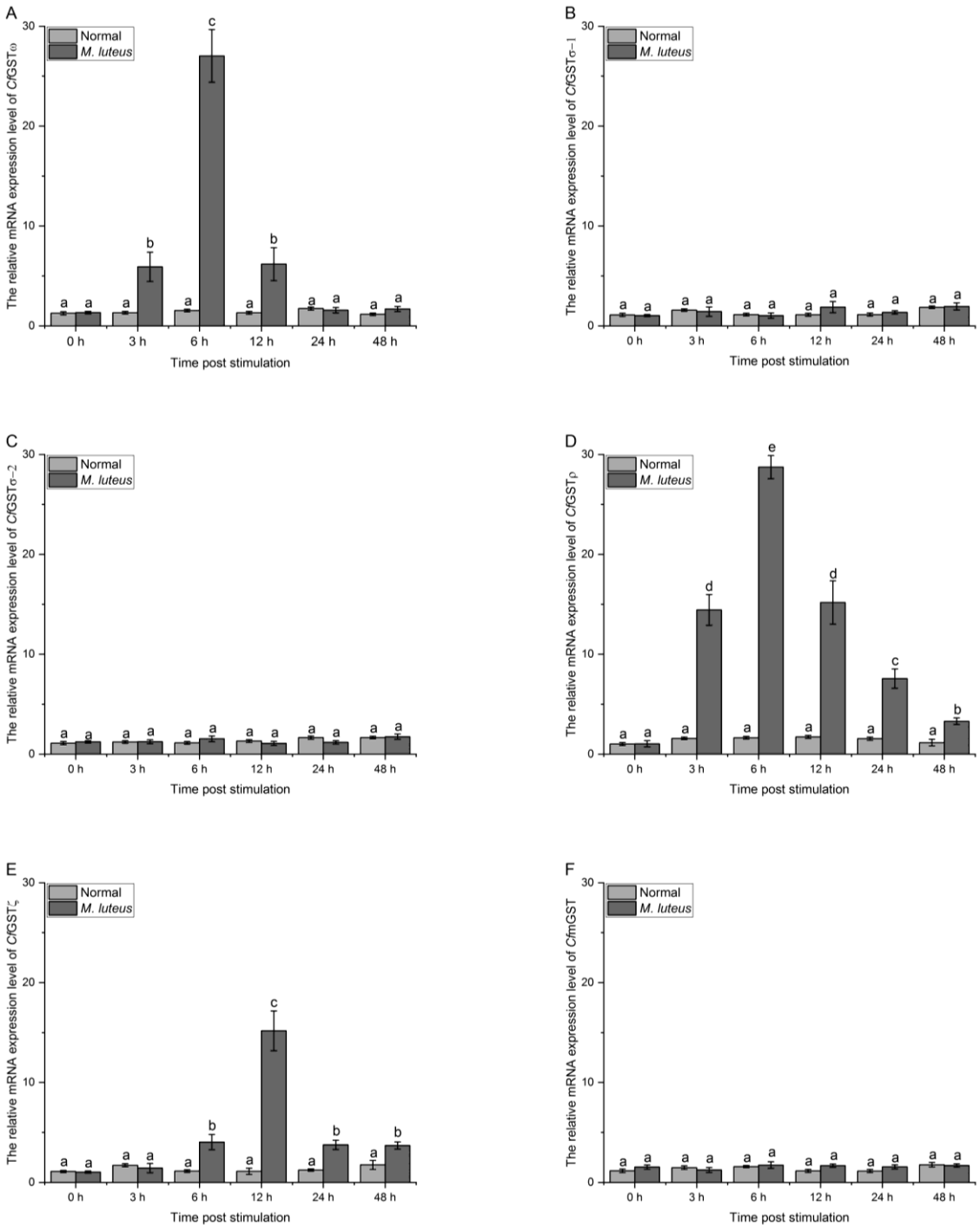

Fig. 6 Temporal mRNA expression profiles of six *Cf*GSTs detected by qRT-PCR in scallop hemocytes post *M. luteus* stimulation (A: *Cf*GSTω, B: *Cf*GSTσ-1, C: *Cf*GSTσ-2, D: *Cf*GSTρ, E: *Cf*GSTζ, F: *Cf*mGST). Each values was shown as mean ± S.D. (n = 5), and bars with different characters indicated significant difference ($p < 0.05$)

performed a crucial role in the detoxification process, while high constitutively expressed GSTs might involve in protecting the cell against endogenous oxidative stress (Zhang *et al*., 2012a). It could be speculated that *Cf*GSTσ-1 perhaps played a pivotal role in the detoxification process. So, we hypothesized based on these results that each of the GST classes with different tissues distributions might be involved in some specific physiological functions in the basal metabolism of scallop.

Mollusks highly rely on innate immunity, and hemocytes-mediated phagocytosis is considered as a main arm of innate immune defense strategies (Song *et al*., 2015; Wang *et al*., 2016a). Infection of microbes could induce hemocytes-mediated phagocytosis accompanied with respiratory burst and

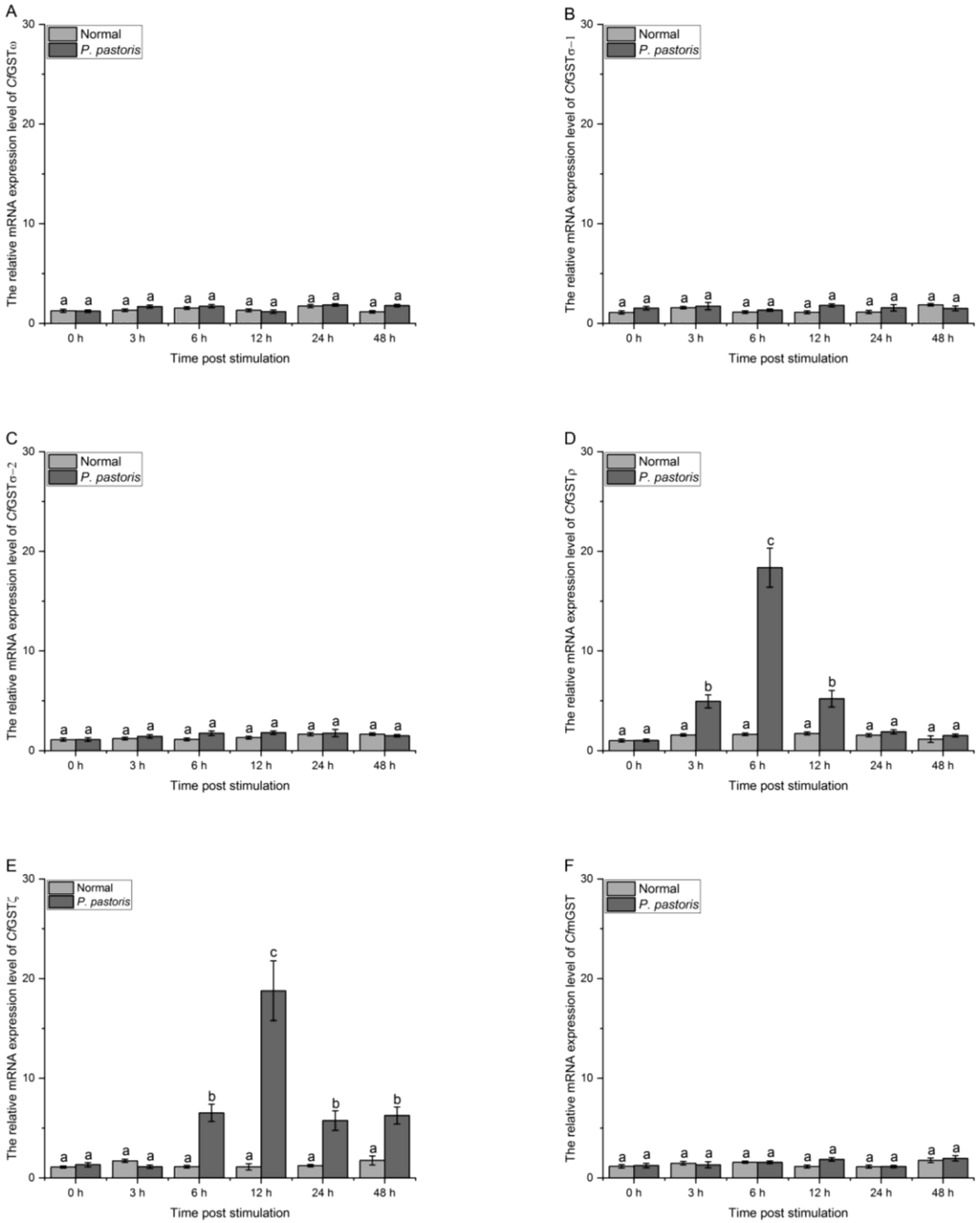

Fig. 7 Temporal mRNA expression profiles of six *Cf*GSTs detected by qRT-PCR in scallop hemocytes post *P. pastoris* stimulation (A: *Cf*GSTω, B: *Cf*GSTσ-1, C: *Cf*GSTσ-2, D: *Cf*GSTρ, E: *Cf*GSTζ, F: *Cf*mGST). Each values was shown as mean ± S.D. (n = 5), and bars with different characters indicated significant difference ($p < 0.05$)

followed by mass production of ROS in various organisms ranging from invertebrate to vertebrate (Halliwell, 2006; Benedetti *et al*., 2015). Compared with vertebrate GSTs, rare information about the mRNA expression profiles of different classes of GSTs is available in mollusks, considering their indispensable roles in antioxidant system (Song *et al*., 2015). In the present study, almost all the identified *Cf*GSTs were high expressed in hemocytes. So this tissue was selected as candidate for investigating the temporal mRNA expression profiles of *Cf*GSTs post various microbe stimulations. Among of the previous identified GSTs from aquatic species, some could be induced by foreign stimulus or invading microbes and be involved in innate immunity (Ren *et al*., 2009; Mu *et al*., 2010; Chen *et al*., 2011; Li *et al*., 2012; Yang *et al*., 2012; Duan *et al*., 2013; Wang *et al*., 2013; Shao *et al*., 2017). In

the present study, it was observed that the mRNA transcripts of these six *Cf*GST genes all drastically increased after one or two kinds of microbe stimulation. For examples, *Cf*GSTσ-1, *Cf*GSTσ-2 and *Cf*mGST could only respond to the stimulation of *V. anguillarum*, while both *Cf*GSTω and *Cf*GSTρ could be significantly induced by two kinds of microbe stimulation, which indicated that they could be involved in the innate immune response of scallop against different invading pathogens. Interestingly, *Cf*GSTζ could respond to all the three kinds of microbe stimulation with similar expression profiles, indicating *Cf*GSTζ was involved in the innate immune responses to more microbes and its modulation to different invading microbes might share the similar mechanism. Similar phenome has been observed in *V. philippinarum*, in which all the *Vp*GSTs showed differential response profiles depending on the concentrations of various toxicants and exposure times. Additionally, *Cf*GSTσ-2 with low basal mRNA expression level responded to invading *V. anguillarum* more rapidly and intensely than *Cf*GSTσ-1, similarly, the basal mRNA expression level of *Es*cytMnSOD in hemocytes was higher than that of *Es*mtMnSOD by approximately two times, which indicated that *Es*cytMnSOD might play a more routine role in the physiological activity of crabs (Wang *et al*., 2015). These differences in their mRNA expression profile indicated that *Cf*GSTσ-1 might play a routine role in the detoxification process, while *Cf*GSTσ-2 would mainly be involved in the response to invading pathogens.

In summary, the full-length cDNA sequences of six GST genes, including *Cf*GSTω, *Cf*GSTσ-1, *Cf*GSTσ-2, *Cf*GSTρ, *Cf*GSTζ and *Cf*mGST, were obtained from *C. farreri*. All the *Cf*GSTs were constitutively expressed in all the tested tissues and they were drastically but differentially induced post different microbe stimulation. Based on these obtained results, it could be hypothesized that *Cf*GSTs were involved in the defense responses of *C. farreri* against bacterial infection. Additionally, the difference in their temporal mRNA expression patterns against various microbe stimulation indicated that *Cf*GSTs would play pivotal but different roles in the innate immune responses of scallop.

Acknowledgement

This research was supported by the National Natural Science Foundation of China (31530069). We are grateful to Prof. Zhaolan Mo, Yellow Sea Fisheries Research Institute, Chinese Academy of Fishery Sciences, for her kindly providing the *V. anguillarum* strain M3, and Dr. Alexia-Ileana Zaromytidou, Springer Nature, for her kindly help in English writing. We would like to thank the editor office and the expert reviewers for their constructive suggestions and enlightening comments during the revision.

References

Benedetti S, Nuvoli B, Catalani S, Galati R. Reactive oxygen species a double-edged sword for mesothelioma. Oncotarget 6: 16848, 2015.

Chen J, Xiao S, Deng Y, Du X, Yu Z. Cloning of a novel glutathione S-transferase 3 (GST3) gene and expression analysis in pearl oyster, *Pinctada martensii*. Fish Shellfish Immunol. 31: 823-830, 2011.

Cong M, Ni D, Song L, Wang L, Zhao J, Qiu L, *et al*. Molecular cloning, characterization and mRNA expression of peroxiredoxin in Zhikong scallop *Chlamys farreri*. Mol. Biol. Rep. 36: 1451-1459, 2009.

Doi A, Pham R, Hughes M, Barber S, Gallagher P. Molecular cloning and characterization of a glutathione S-transferase from largemouth bass (*Micropterus salmoides*) liver that is involved in the detoxification of 4-hydroxynonenal. Biochem. Pharmacol. 67: 2129-2139, 2004.

Duan Y, Liu P, Li J, Li J, Chen P. Expression profiles of selenium dependent glutathione peroxidase and glutathione S-transferase from *Exopalaemon carinicauda* in response to *Vibrio anguillarum* and WSSV challenge. Fish Shellfish Immunol. 35: 661-670, 2013.

Halliwell B. Reactive species and antioxidants. Redox biology is a fundamental theme of aerobic life. Plant Physiol. 141: 312-322, 2006.

Harris E. Regulation of antioxidant enzymes. FASEB J. 6: 2675-2683, 1992.

Hayes J, Flanagan J, Jowsey I. Glutathione transferases. Annu. Rev. Pharmacol 45: 51-88, 2005.

He C, Klionsky D. Regulation mechanisms and signaling pathways of autophagy. Annu. Rev. Genet. 43: 67-93, 2009.

Hoffmann J, Kafatos F, Janeway C, Ezekowitz R. Phylogenetic perspectives in innate immunity. Science 284: 1313-1318, 1999.

Jia Z, Wang M, Wang X, Wang L, Qiu L, Song L. Transcriptome sequencing reveals the involvement of reactive oxygen species in the hematopoiesis from Chinese mitten crab *Eriocheir sinensis*. Dev. Comp. Immunol. 82: 94-103, 2018.

Lee Y, Lee K, Park H, Park H, Raisuddin S, Ahn I, *et al*. Sequence, biochemical characteristics and expression of a novel Sigma-class of glutathione S-transferase from the intertidal copepod, *Tigriopus japonicus* with a possible role in antioxidant defense. Chemosphere 69: 893-902, 2007.

Li C, Ni D, Song L, Zhao J, Zhang H, Li L. Molecular cloning and characterization of a catalase gene from Zhikong scallop *Chlamys farreri*. Fish Shellfish Immunol. 24: 26-34, 2008.

Li C, Su X, Li Y, Li T, Sun C, Zhou T, *et al*. Two classes of glutathione S-transferase genes with different response profiles to bacterial challenge in *Venerupis philippinarum*. Fish Shellfish Immunol. 32: 219-222, 2012.

Li F, Wu H, Wang Q, Li X, Zhao J. Glutathione S-transferase (GST) gene expression profiles in two marine bivalves exposed to BDE-47 and their potential molecular mechanisms. Chin. J. Oceanol. Limnol. 33: 705-713, 2015.

Li Y, Song X, Wang W, Wang L, Yi Q, Jiang S, *et al*. The hematopoiesis in gill and its role in the immune response of Pacific oyster *Crassostrea gigas* against secondary challenge with *Vibrio splendidus*. Dev. Comp. Immunol. 71: 59-69, 2017a.

Li Y, Sun X, Hu X, Xun X, Zhang J, Guo X, *et al*. Scallop genome reveals molecular adaptations to semi-sessile life and neurotoxins. Nat. Commun. 8: 1721, 2017b.

Li Z, Chen R, Zuo Z, Mo Z, Yu A. Cloning, expression and identification of two glutathione S-transferase isoenzymes from *Perna viridis*. Comp. Biochem. Phys. B 165: 277-285, 2013.

Liu J, Pan L, Zhang L, Miao J, Wang J. Immune responses, ROS generation and the haemocyte damage of scallop *Chlamys farreri* exposed to Aroclor 1254. Fish Shellfish Immunol. 26: 422-428, 2009.

Martindale J, Holbrook N. Cellular response to oxidative stress: signaling for suicide and survival. J. Cell. Physiol. 192: 1-15, 2002.

Miao J, Pan L, Liu N, Xu C, Zhang L. Molecular cloning of CYP4 and GSTpi homologues in the scallop *Chlamys farreri* and its expression in response to benzo [a] pyrene exposure. Mar. Genom. 4, 99-108, 2011.

Morgenstern R, Guthenberg C, Depierre J. Microsomal Glutathione S-Transferase. Eur. J. Biochem. 128: 243-248, 1982.

Mu C, Ni D, Zhao J, Wang L, Song L, Li L, *et al*. cDNA cloning and mRNA expression of a selenium-dependent glutathione peroxidase from Zhikong scallop *Chlamys farreri*. Comp. Biochem. Phys. B 157: 182-188, 2010.

Ni D, Song L, Gao Q, Wu L, Yu Y, Zhao J, *et al*. The cDNA cloning and mRNA expression of cytoplasmic Cu, Zn superoxide dismutase (SOD) gene in scallop *Chlamys farreri*. Fish Shellfish Immunol. 23: 1032-1042, 2007.

Ren H, Xu D, Gopalakrishnan S, Qiao K, Huang W, Wang K. Gene cloning of a sigma class glutathione S-transferase from abalone (*Haliotis diversicolor*) and expression analysis upon bacterial challenge. Dev. Comp. Immunol. 33: 980-990, 2009.

Sandamalika W, Priyathilaka T, Liyanage D, Lee S, Lim H, Lee J. Molecular characterization of kappa class glutathione S-transferase from the disk abalone (*Haliotis discus discus*) and changes in expression following immune and stress challenges. Fish Shellfish Immunol. 77: 252-263, 2018.

Schmittgen T, Livak K. Analyzing real-time PCR data by the comparative C_T method. Nat. Protoc. 3: 1101-1108, 2008.

Shao Y, Lv Z, Li C, Zhang W, Duan X, Qiu Q, *et al*. Molecular cloning and functional characterization of theta class glutathione S-transferase from *Apostichopus japonicus*. Fish Shellfish Immunol. 63: 31-39, 2017.

Song L, Wang L, Zhang H, Wang M. The immune system and its modulation mechanism in scallop. Fish Shellfish Immunol. 46: 65-78, 2015.

Strange R, Spiteri M, Ramachandran S, Fryer A. Glutathione-S-transferase family of enzymes. Mutat. Res-Fund. M. 482: 21-26, 2001.

Wan Q, Whang I, Lee J. Molecular cloning and characterization of three sigma glutathione S-transferases from disk abalone (*Haliotis discus discus*). Comp. Biochem. Physiol. B. 151: 257-267, 2008.

Wang C, Zhao J, Mu C, Wang Q, Wu H, Wang C. cDNA cloning and mRNA expression of four glutathione S-transferase (GST) genes from *Mytilus galloprovincialis*. Fish Shellfish Immunol. 34: 697-703, 2013.

Wang L, Song L, Zhao J, Qiu L, Zhang H, Xu W, *et al*. Expressed sequence tags from the Zhikong scallop (*Chlamys farreri*): discovery and annotation of host-defense genes. Fish Shellfish Immunol. 26: 744-750, 2009.

Wang M, Wang B, Jiang K, Liu M, Shi X, Wang L. A mitochondrial manganese superoxide dismutase involved in innate immunity is essential for the survival of *Chlamys farreri*. Fish Shellfish Immunol. 72: 282-290, 2018.

Wang M, Wang B, Liu M, Jiang K, Wang L. Sequence features, expression profiles and biochemical characteristics of a sigma class glutathione S-transferase gene (AiGSTσ) from bay scallop *Argopecten irradians*. ISJ - Invert. Surv. J. 14: 522-533, 2017a.

Wang M, Wang L, Yi Q, Gai Y, Song L. Molecular cloning and characterization of a cytoplasmic manganese superoxide dismutase and a mitochondrial manganese superoxide dismutase from Chinese mitten crab *Eriocheir sinensis*. Fish Shellfish Immunol. 47: 407-417, 2015.

Wang M, Wang L, Guo Y, Yi Q, Song L. An LRR-only protein representing a new type of pattern recognition receptor in *Chlamys farreri*. Dev. Comp. Immunol. 54: 145-155, 2016a.

Wang M, Wang L, Jia Z, Wang X, Yi Q, Lv Z, *et al*. The versatile functions of LRR-only proteins in mollusk *Chlamys farreri*. Dev. Comp. Immun. 77: 188-199, 2017b.

Wang M, Wang L, Xin L, Wang X, Wang L, Xu J, *et al*. Two novel LRR-only proteins in *Chlamys farreri*: Similar in structure, yet different in expression profile and pattern recognition. Dev. Comp. Immun. 59: 99-109, 2016b.

Xu C, Pan L, Liu N, Wang L, Miao J. Cloning, characterization and tissue distribution of a pi-class glutathione S-transferase from clam (*Venerupis philippinarum*): Response to benzo [α] pyrene exposure. Comp. Biochem. Physiol. C 152: 160-166, 2010.

Yang J, Wei X, Xu J, Yang D, Liu X, Yang J, *et al*. A sigma-class glutathione S-transferase from *Solen grandis* that responded to microorganism glycan and organic contaminants. Fish Shellfish Immunol. 32: 1198-1204, 2012.

Zhang L, Qiu L, Wu H, Liu X, You L, Pei D, *et al*. Expression profiles of seven glutathione S-transferase (GST) genes from *Venerupis philippinarum* exposed to heavy metals and benzo [a] pyrene. Comp. Biochem. Physiol. C 155: 517-527, 2012a.

Zhang L, Wu H, Liu X, Chen L, Wang Q, Zhao J, *et al*. Molecular cloning and differential expression patterns of sigma and omega glutathione S-transferases from *Venerupis philippinarum* to heavy metals and benzo a pyrene exposure. Chin. J. Oceanol. Limnol. 30: 413-423, 2012b.

Zhang Z, Lv Z, Shao Y, Qiu Q, Zhang W, Duan X, *et al*. Microsomal glutathione transferase 1 attenuated ROS-induced lipid peroxidation in *Apostichopus japonicus*. Dev. Comp. Immunol.

73: 79-87, 2017a.
Zhang Z, Lv Z, Wei Z, Li C, Shao Y, Zhang W, *et al*. Microsomal glutathione transferase 2 modulates LTC4 synthesis and ROS production in *Apostichopus japonicus*. Mol. Immunol. 91: 114-122, 2017b.